Applied Surface Science 615 (2023) 156315

Contents lists available at ScienceDirect

Applied Surface Science

journal homepage: www.elsevier.com/locate/apsusc

Full Length Article

Graphene oxide-mediated copper reduction allows comparative evaluation of oxygenated reactive residues exposure on the materials surface in a simple one-step method

Valentina Palmieri [a,b,*], Francesco Amato [c], Andrea Giacomo Marrani [c,*], Ginevra Friggeri [d], Giordano Perini [b,d], Alberto Augello [b], Marco De Spirito [b,d], Massimiliano Papi [b,d]

[a] Istituto dei Sistemi Complessi, CNR, Via dei Taurini 19, 00185 Rome, Italy
[b] Fondazione Policlinico Universitario A. Gemelli IRCSS, 00168 Rome, Italy
[c] Dipartimento di Chimica, Università degli Studi di Roma "La Sapienza", p.le Aldo Moro 5, I-00185 Roma, Italy
[d] Dipartimento di Neuroscienze, Università Cattolica del Sacro Cuore, Largo Francesco Vito 1, 00168 Rome, Italy

ARTICLE INFO

Keywords:
Graphene
Surface group
Scaffold
Composites
Method

ABSTRACT

Graphene Oxide (GO) is the oxidized form of graphene rich in surface groups comprising carbonyl, carboxyl, hydroxyl, and epoxy residues. The solubility in water makes GO an ideal material in the biomedical field though the plethora of synthesis methods available can modify the balance of oxygen groups and, consequently, the effects on eukaryotic and prokaryotic cells. For this reason, GO materials are always characterized with spectroscopic methods such as X-ray photoelectron and Fourier-transform Infrared spectroscopy. However, these techniques have some limitations, being disruptive and not clearly indicating oxygen functionalities available to react with polymers or biological media.

In this work, we exploit GO reactivity with copper ions to develop a colorimetric method for the facile evaluation of surface oxidation degree and accessibility in polymeric samples. In the presence of GO, Cu^{2+} is reduced to Cu^{1+} and can react with bicinchoninic acid and induce light absorption at 562 nm. We observed that this reaction is dependent both on concentration and oxidation degree, and can be used to estimate GO exposure in thick composite samples. This technique will be fundamental in the future for scaffold characterization in tissue engineering and all the surface science studies analyzing GO-related materials' interactions with biological entities.

1. Introduction

Graphene is an allotrope of carbon known for its bidimensional honeycomb configuration that causes unique interactions with eukaryotic and prokaryotic cells. Graphene-based materials have been exploited in biomaterial science, optics and electronics, and many other fields of research, including 3D printing and diagnostics [1–4]. Graphene oxide (GO), the oxidized derivative of graphene, has been investigated mainly in the last 10–15 years. The surface of this bidimensional material consists of several chemical groups comprising carbonyl (CO), carboxyl (COOH), hydroxyl (COH), and epoxy (COC). These groups which can be quantified by X-ray photoelectron spectroscopy (XPS) and Fourier-transform Infrared (FT-IR) spectroscopy[5,6]. The GO oxygen groups' amount and quality can be varied by several reduction methods, to modify surface availability and, consequently, biological effects. Indeed, the attachment of macromolecules such as proteins and carbohydrates to GO is influenced by charge and steric hindrance of functional groups[7]. Since prokaryotic and eukaryotic cells respond to the adsorbed macromolecules, oxygen groups will eventually determine GO effects on bacteria and human cells in biological media[7–9].

A clear example of how oxygen influences the biological effects of GO comes from the evaluation of differentiation of human mesenchymal stem cells (MSCs) seeded on either graphene or GO substrates[10,11]. Indeed, the strong binding of insulin in the cell growth medium exhibited by graphene induces insulin degradation and causes acceleration of MSCs differentiation toward the osteogenic line and suppression

* Corresponding authors at: Istituto dei Sistemi Complessi, CNR, Via dei Taurini 19, 00185 Rome, Italy (V. Palmieri). Dipartimento di Chimica, Università degli Studi di Roma "La Sapienza", p.le Aldo Moro 5, I-00185 Roma, Italy (A.G. Marrani).
E-mail addresses: valentina.palmieri@cnr.it, andrea.marrani@uniroma1.it (A.G. Marrani).

https://doi.org/10.1016/j.apsusc.2022.156315
Received 4 November 2022; Received in revised form 22 December 2022; Accepted 31 December 2022
Available online 3 January 2023

of adipocyte production[10]. Differently, GO electrostatic binding to insulin, due to functional groups, avoids any interference with the adipogenesis process, thanks to the preservation of insulin 3D structure [10]. Bacteria also react differently to graphene or GO surfaces[12]. As recently demonstrated by Henriquez and colleagues, clinically relevant bacteria adhere less to GO, while are more viable on reduced GO (rGO), which is similar to graphene[13]. The effects on microorganisms are largely dependent on bacteria strain, but are in any case influenced by the amount of oxygen available on surface[13].

The oxygen groups on GO also act as a bridge in composites for tissue engineering scaffold production. The most common fabrication technique for GO-composite production envisages the mixing of GO with a matrix monomer or pre-polymer, followed by polymerization initiated by heat or radiation[14]. This method produces both covalent and noncovalent interactions between the GO oxygen-containing groups and the polymer matrix, which enhances the properties of the composites or 3D printing inks [14]. In these composite materials, the availability of oxygen groups is strictly dependent on the extent of the polymerization reaction. Consequently, also the scaffolds effects on biological entities, i.e. cells or microorganisms, depends on the number of oxygen groups that reacted during polymerization.

These pieces of evidence highlight the biological importance of quantification of reactive oxygen groups on the surface, though the calculation of the exact amount of these groups is a challenging issue. The presence of oxygen functional groups is measured by XPS or FT-IR, which are gold-standard chemical spectroscopy techniques. Despite being informative, these techniques are disruptive and the quality of measurement interpretation can be affected by the sample. Indeed, data can be misinterpreted as the vibration/rotation modes of some functional groups overlap (FT-IR), or their binding energies are so close that theoretical deconvolution is necessary (XPS) [15]. In the end, these techniques are limited when it is required to evaluate GO groups availability in thick 3D supports like in 3D printed scaffold production [16].

In this paper, we propose a quick method to assess the surface availability of oxygen groups on GO-based materials using the ability of GO to interact with Cu^{2+} ions and detecting the interaction of freshly formed Cu^{+} with bicinchoninic acid (BCA) via UV–vis spectroscopy. In fact, in the presence of Cu^{+} ions in solution, a Cu^{+}-BCA complex is formed, resulting in a strong absorbance at 562 nm[17]. Here, we show how GO samples with different amounts of oxygenated groups on surface either in soluble form, as coatings or in composite 3D scaffolds interact with Cu^{2+} ions and reduce them to Cu^{+} according to the oxygen groups accessibility to the solvent. Consequently, the copper colorimetric reaction with BCA represents a one-step method extremely useful to compare different samples for material science and scaffold design.

2. Materials and methods

Graphene nanoplatelets provided by Directa Plus will be referred to as **G** sample and dissolved in ddH_2O.

GO-1 indicates a graphene oxide material synthesized by a procedure reported in the literature, with some modifications[18,19]. Briefly, 69 mL of H_2SO_4 (96 wt%) were added to a mixture of synthetic graphite (3.0 g) and $NaNO_3$ (1.5 g) and the mixture was cooled at 0 °C. Then, $KMnO_4$ (9.0 g) was added in portions and the mixture was stirred at 35 °C for 30 min. Subsequently, distilled water (138 mL) was added slowly and the mixture was heated at 98 °C for 15 min. Next, additional distilled water (420 mL) and H_2O_2 (3 mL, 30 % v/v) were added. For workup, a filtration through a filter paper was performed and the solid obtained was centrifuged at 4000 rpm for 30 min in presence of HCl 1.12 M and distilled water (four times). During this step of purification, the supernatant was whenever discharged away and replaced with distilled water. Next, the solid was transferred in a round-bottom flask, then distilled water was added, and the mixture was stirred for a night to ensure a proper exfoliation. Next, the dispersion was sonicated for 30 min and centrifuged at 3000 rpm for 40 min in order to recover the yellowish supernatant and discharge, as precipitate, the graphite oxide that may be present. This procedure was repeated until the obtainment of an almost colorless supernatant. Finally, the dispersion of **GO-1** was dried under vacuum by means of a rotavapor at 35.0 °C and the solid powder stored in a desiccator.

GO-2 represents a graphene oxide material synthesized by a similar procedure as the previous one, but with some modifications[18]. In particular, a mixture of concentrated H_2SO_4/H_3PO_4 (9:1, namely 360:40 mL) were added to a mixture of synthetic graphite (3.0) and $KMnO_4$ (18.0 g). The mixture was then heated at 50 °C for 15 h. After this time, the mixture was cooled at room temperature (r.t.) and poured onto ice (400 mL) with H_2O_2 (3 mL, 30 % v/v). For workup, filtration through a filter paper was performed and the solid collected was centrifuged at 4000 rpm for 30 min in the presence of HCl 1.12 M and distilled water (four times). During this step of purification, the supernatant was whenever discharged away and replaced with distilled water. Finally, the dispersion of **GO-2** was dried under vacuum by means of a rotavapor at 35.0 °C and the solid powder stored in a desiccator.

Polycaprolactone (**PCL)-GO** and poly(lactic-*co*-glycolic acid) **(PLGA)-GO** have been produced by dissolving the corresponding polymers and GO-1 (2 wt%) in dichloromethane (DCM), stirring the samples for 2 h, drop casting the composites on glass slides and letting evaporate the solvent overnight.

Infrared spectra were recorded on a Varian FT-IR 660 instrument in the range of 4000–500 cm^{-1} with a spectral resolution of 4 cm^{-1} and 32 scans in KBr pellets.

Raman spectra were run at r.t. in backscattering geometry with an inVia Renishaw micro-Raman spectrometer equipped with an air-cooled CCD detector and super-Notch filters. An Ar^{+} ion laser ($\lambda_{laser} = 514$ nm) was used, coupled to a Leica DLML microscope with a 20 × objective. The resolution was 2 cm^{-1} and spectra were calibrated using the 520.5 cm^{-1} line of a silicon wafer. Raman spectra were acquired in several (6–10) different spots on the surface of the samples. For GO-1 and GO-2, each spectrum was acquired with 1 % of power, 10 s of spectral acquisition and 20 scans.

XPS measurements were carried out using a modified Omicron NanoTechnology MXPS system equipped with a monochromatic Al Kα ($h\nu = 1486.7$ eV) X-ray source (Omicron XM-1000), operating the anode at 14 kV and 16 mA. The C1s photoionization region was acquired using an analyzer pass energy of 20 eV, while the survey spectra were acquired with a pass energy of 50 eV. A take-off angle of 21° with respect to the sample surface normal was adopted. The experimental spectra were theoretically reconstructed by fitting the secondary electrons background to a Shirley function and the elastic peaks to pseudo-Voigt functions described by a common set of parameters: position, full-width at half-maximum (FWHM), Gaussian-Lorentzian ratio. The relative amount of the different oxygenated functional groups was determined through the area of the peaks within the curve fitting envelope of the C 1 s region, with an uncertainty of ± 10 %. The contribution from sp^2 C atoms in the C═C network (peak at 284.8 eV) was set as a binding energy reference. Atomic Force Microscopy images were obtained by 100 μL of each sample (10 μg/mL) deposited on sterile mica slides and air-dried overnight. Images were acquired with a NanoWizard II (JPK Instruments AG, Berlin, Germany) using silicon cantilevers with high aspect-ratio conical silicon tips (CSC36 Mikro-Masch, Tallinn, Estonia) characterized by an end radius of about 10 nm, a half conical angle of 20°, and a spring constant of 0.6 N/m.

2.1. Cu^{2+} reduction assessment by UV-spectroscopy

Bicinchoninic acid (BCA), Cu^{2+}, and other buffer solutions were purchased from Euroclone as a part of the BCA micro assay kit. For each reaction, the reagents have been mixed according to the manufacturer specification. For the quantification of the BCA interaction with graphene, a first set of experiments has been performed without Cu^{2+} in the

mixture. After 2 h of incubation at 37 °C, the formation of the complex Cu^{+} and BCA has been investigated by spectroscopy. Absorption spectra were obtained by using a Cytation 3 Cell Imaging Multi-Mode Reader (Biotek, Canada) at wavelengths from 230 to 700 nm with a step of 2 nm in 96-wells. Measurements have been done in triplicate. Data from blank samples containing either water with BCA and Cu^{2+} or G/GO-1/GO-2 alone were acquired for proper spectra subtraction.

3. Results and discussion

To analyze graphene materials reactivity with Cu^{2+}, we have used three graphene-based materials, namely G, GO-1 and GO-2, bearing different amounts of oxygenated surface groups. In particular, G represents graphene nanoplatelets, while GO-1 and GO-2 are graphene oxides synthesized to obtain a medium or high amount of oxygenated groups concentration on the surface, respectively. We have characterized each material by means of AFM, FT-IR, Raman and XPS spectroscopy. AFM demonstrates the monolayer nature of GO-1 and GO-2 and the higher thickness of G nanoplatelets, which are few layers nanoparticles and tend also to aggregate in water (Fig. 1).

GO-derived materials display infrared-active vibrational modes owing to the presence of oxygen-based functional groups. In particular, the FT-IR spectrum (Fig. 2a, black line) of GO-1 prepared by following the classical Hummers' procedure[20], shows a broad band observed at 3600–2400 cm^{-1} relative to the stretching modes of O—H bonds derived from water molecules intercalated in its structure. Another band centered at ≈1720 cm^{-1} is ascribable to the stretching mode of C═O bonds of carboxyl, ketone and aldehyde groups in addition to another one at ≈1619 cm^{-1} which is assigned to the bending mode of adsorbed water molecules. Finally, the band localized at ≈1220 cm^{-1}, could be relative to the C—O—C vibration of epoxides even if this attribution is still debated[21]. Conversely, the FT-IR spectrum of GO-2 (Fig. 2a, red line) synthesized in presence of H_3PO_4, provides a very intense additional band centered at ≈1125 cm^{-1} which could be attributed to the abundance of C—O bonds of oxygen-based functionalities (epoxy, C-OH) [22]. Finally, the FT-IR spectrum of G (Fig. 2a, blue line), does not show any signal, as expected in the absence of polar groups.

Raman spectroscopy was applied to all samples, and the recorded spectra (Fig. 2b) display the peculiar bands D and G centered at ≈1360 and ≈1600 cm^{-1}, for the GO-1 and GO-2 samples, confirming their graphene oxide characteristics. Notably, the recorded spectra are closely comparable and show a D/G band intensity ratio (I_D/I_G) of 0.83, in full accordance with literature value for similar systems[18]. Conversely, the spectrum of G (Fig. 2b, blue line), displays the typical Raman features of graphene nanoplatelets, namely the G band localized at ≈1576 cm^{-1} and the weaker D band at ≈1350 cm^{-1}.

The samples were subject to XPS analysis to gain further insight on the oxidation degree and chemical composition (Fig. 3).

Fig. 3 shows the XPS spectra in the C 1 s photoionization region for the **G**, **GO-1** and **GO-2** samples (Fig. 3a, b and c, respectively) investigated in this work. The C 1 s spectrum of G sample shows the typical lineshape and position of a purely graphite-like sample, with a main component at 284.1 eV and an asymmetric tail at the high BE side of the main peak, as expected for metalloid systems with a continuum of electron density of states just above the Fermi level [23,24]. As expected, this material is substantially lacking of oxygenated functional groups. Spectra b and c, respectively refer to the GO-1 and GO-2 samples, which display a series of chemically shifted components, as evidenced by the curve-fitting procedure. As we previously reported for similar systems[25–30], these complex envelope is due to the presence

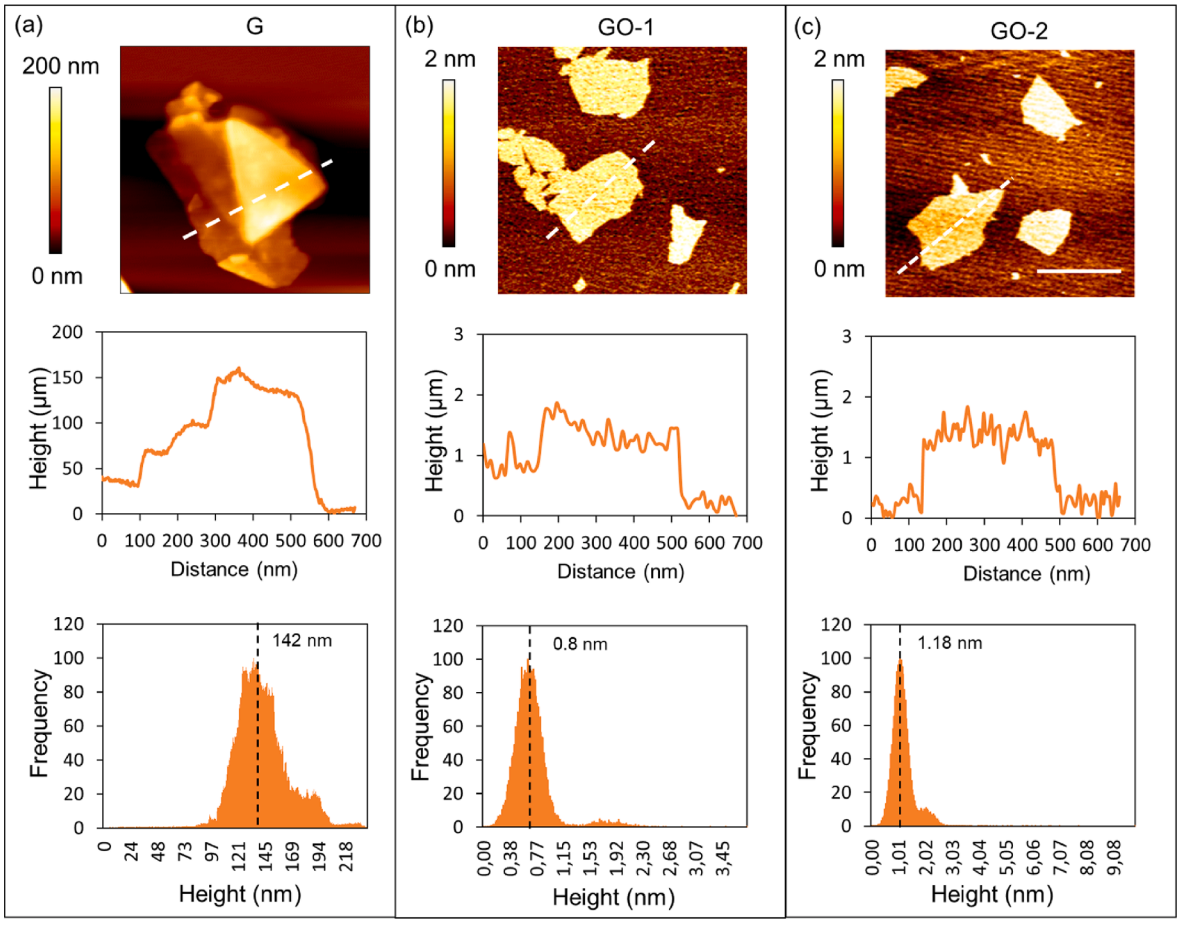

Fig. 1. AFM images of G (a), GO-1 (b) and GO-2 (c). For each sample a representative height profile and the histogram of height frequency is reported.

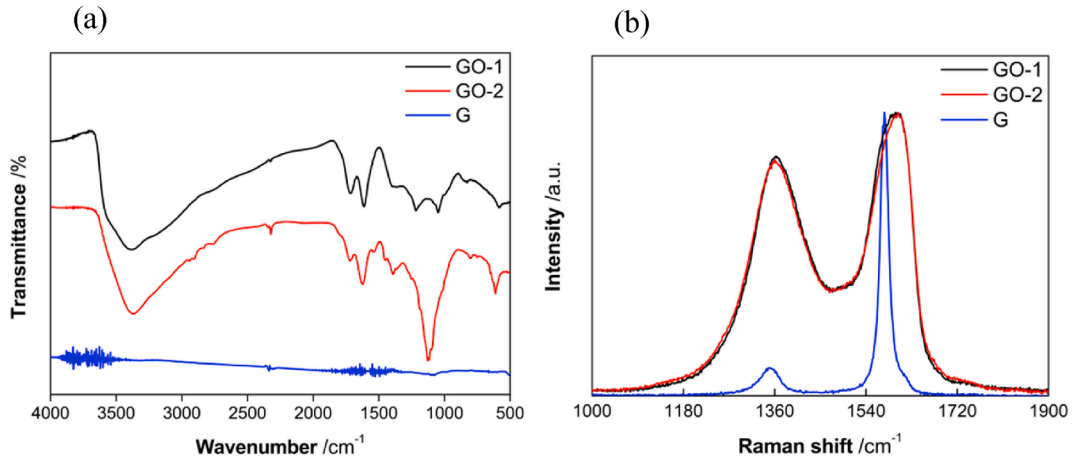

Fig. 2. (a) FT-IR and (b) Raman spectra of GO-1, GO-2 and G samples.

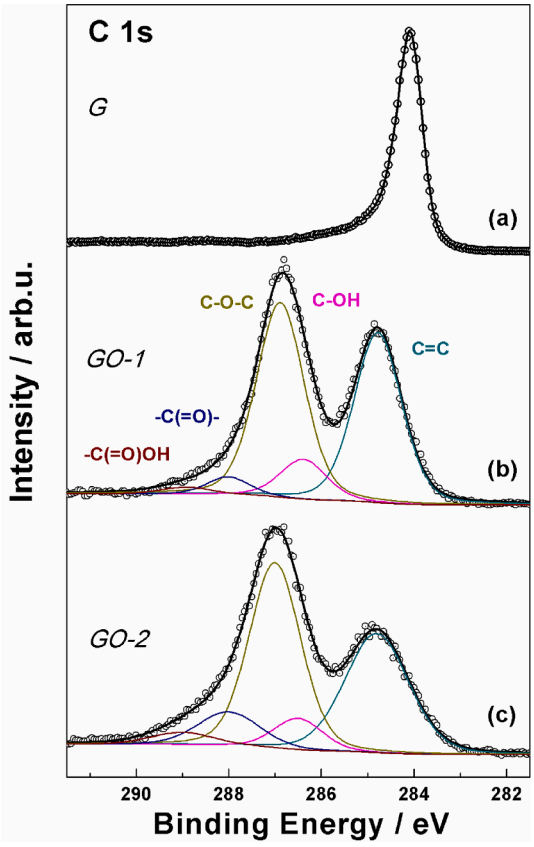

Fig. 3. C 1 s XPS spectra of (a) G, (b) GO-1 and (c) GO-2 samples. Experimental data are reported in dots, while curve-fitting results are represented with colored continuous lines.

of oxygenated functional groups both at the edges and basal plane of the graphene oxide materials. In particular, the peak at 284.8 eV (dark cyan line in Fig. 4) is assigned to localized C═C bonds or confined C═C islands within the oxygenated carbon network of GO[31,32] while the peaks at 286.5 (magenta), 286.90 (dark yellow), 288.0 (blue) and 289.00 eV (wine) are respectively associated to hydroxyl (C-OH), epoxy (C—O—C), carbonyl (C═O) and carboxyl (COOH) groups[25–29]. According to the area of the peaks resulting from curve-fitting (see Table 1), it is evident that in both GO-1 and GO-2 samples the epoxy moiety is the most abundant among the oxygenated functions at the surface of GO, as generally expected from a Hummers preparative method[20]. The GO-2 sample, which was obtained according to an improved Hummers method following the recipe by Marcano et al.[18], displays a higher oxidation degree than GO-1, as demonstrated by the comparison between the $R_{O/C}$ (oxygen-to-carbon ratio) values of the two samples, determined by XPS (0.46 for GO-2 vs 0.39 for GO-1, see Table 1 and equation reported therein). This behaviour is in full accord with the reference literature [18].

To evaluate G, GO-1 and GO-2 ability to reduce Cu^{2+}, we have used two different experimental setups (Fig. 4). In the first, we have incubated each type of graphene with BCA and Cu^{2+} solutions, then graphene has been removed by centrifugation. In the second setup, we have evaluated graphenes reaction with the BCA alone, to exclude possible material nanosheets complexation with the acid. Also in this case, graphene nanoflakes have been removed by centrifugation and the supernatant was analyzed by spectrophotometry (Fig. 4a). All experiments have been performed in triplicate using a serial dilution of soluble graphene samples (in ddH_2O) and substracting graphene alone as blank.

The results of graphene incubation at different concentrations with BCA and Cu^{2+} solutions are reported in Fig. 4b. Each material was analysed in a concentration range comprised between 31,25 μg/mL and 250 μg/mL. Supernatant absorption has been evaluated at a wavelength of 562 nm. As it is visible, the higher oxidation of GO surface induces a higher signal proportional to the material concentration. The G nanoplatelets showed poor reaction with BCA and Cu^{2+} and a higher propensity to precipitation due to their high hydrophobicity.

We have fitted each curve with a linear equation and obtained m coefficient of 0.0026 ± for GO-2, 0.0014 ± for GO-1 and a flat curve and m ~ 0. for G. These results well correlate with the higher oxidation degree displayed by GO-2 with respect to GO-1 upon XPS investigation (Fig. 3, Table 1). To exclude that the colorimetric reaction was caused by graphenic materials interaction with the acid, we have quantified the signal from the supernatants from samples where Cu^{2+} was not included in the reaction mixture (Fig. 4c). Experiments without Cu^{2+} in solution did not show any absorption peak from the supernatant, indicating a lack of reaction of the BCA and a lack of development of color in the solution. In Fig. 4D, we report a scheme of the whole reaction.

Since G and GO are widely used for composites production and the availability of oxygen groups influences cell and bacteria responses to the material, we have also tested our technique with surfaces of PCL and PLGA with or without GO-1 in the mixture used to mold the samples. We have used a GO-1 mass concentration of 2 %, which is known to be biocompatible with different cell lines[33,34]. In this case, the centrifugation of the reactive media was not necessary, since the graphenic materials were embedded in the bulk of the polymer solution and we were interested in analyzing their surface properties.

Experimental procedure and results are reported in Fig. 5a and 5b,

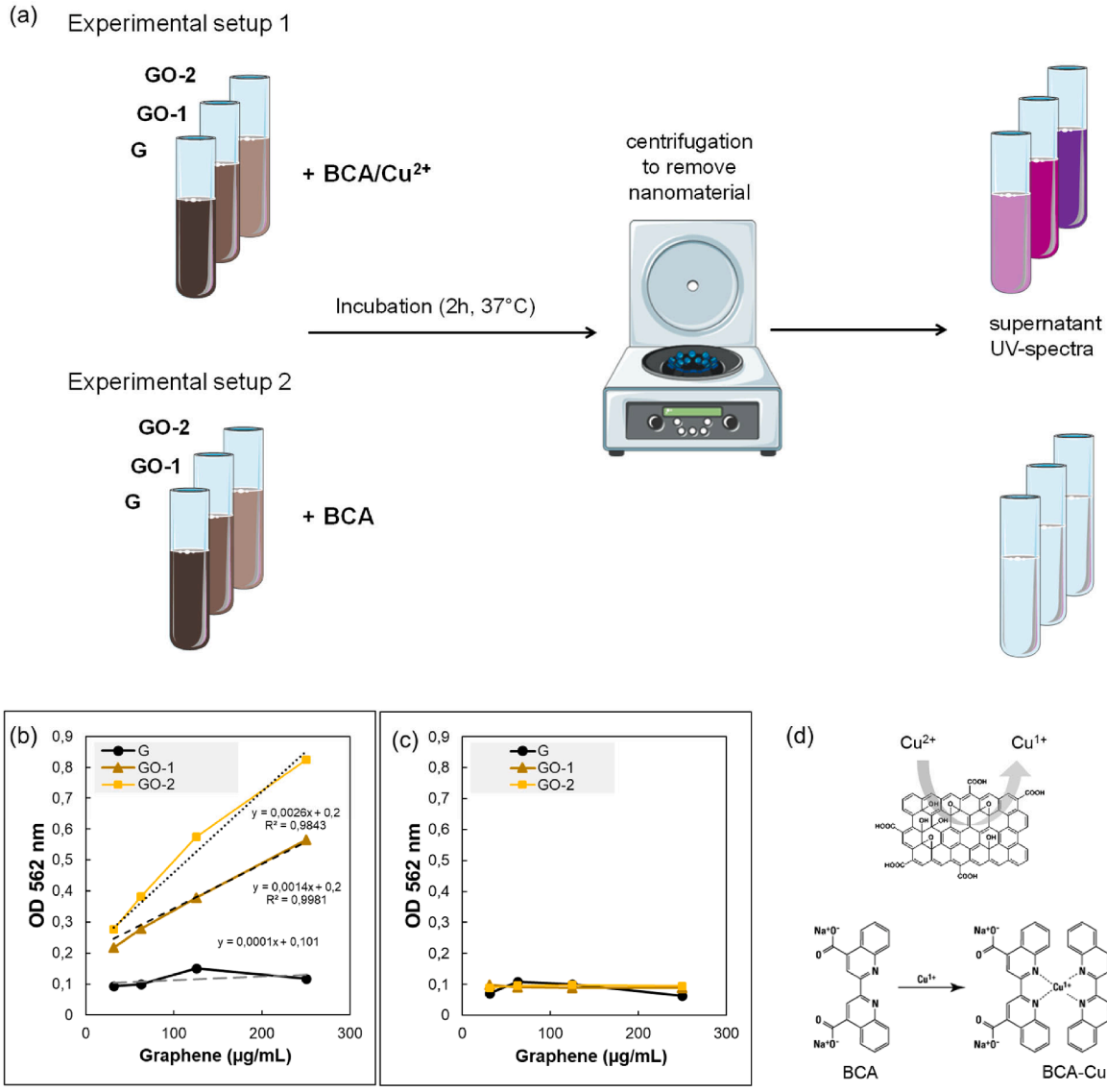

Fig. 4. (a) Experimental setup used to verify G, GO-1 and GO-2 interaction with Cu^{2+}, after incubation for 2 h at 37 °C samples are centrifugated and OD from supernatants is measured. As a control, samples without Cu^{2+} have also been evaluated. **OD from supernatants of each sample with Cu^{2+} and BCA in the mixture (b) or with only BCA (c).** Samples have been tested at different concentrations and data have been fitted with linear equations. Without copper a lack of signal has been recorded after samples centrifugation **(d) Schematic representation of the observed reactions.**

Table 1
Area[a] of relevant oxygenated functional groups in GO samples[b] obtained from XPS C 1 s spectra[c]. $R_{O/C}$ ratio is also reported.[d]

Sample	C-OH	C—O—C	C═O + COO^-	COOH	$R_{O/C}$
GO-1	0.23	1.14	0.09	0.04	0.39
GO-2	0.20	1.25	0.27	0.10	0.46

[a]Normalized to C_{sp2} component.
[b]Sample G is not reported, since it displayed negligible oxidation.
[c]Associated error is ± 10 %.
[d]As estimated by the equation reported here below, where P represents the area of the various C components.

$$R_{O/C} = \frac{P_{C-OH} + 1/2P_{Epoxide} + P_{C=O} + 2P_{COOH}}{P_{C=C} + P_{C-OH} + P_{Epoxide} + P_{C=O} + P_{COOH}}$$

respectively. Even a small amount of GO in the composite (i.e. 2 %) was able to reduce Cu^{2+} to Cu^{+} and changed the BCA reactivity, as shown in the histogram. The absorption signal reflects the reactivity of GO residues available on the scaffold surface, with the PCL-GO sample being more reactive compared to PLGA-GO. This behaviour is fully coherent with the already reported effects that these type of materials exert on eukaryotic cells [33,34], and supports a higher oxygen groups availability in GO when the scaffold is made of PCL. This proof of concept demonstrates the technique's applicability in the field of scaffold design and tissue engineering, since it allows for a quick and easy comparison between different samples.

4. Conclusions

Functional materials and graphene composites are employed in many fields of science, from electronics to bioengineering [3,35–37]. In biological sciences, the oxidized form of graphene, GO, has been largely used for its increased solubility in water and buffer. GO synthesis and subsequent reduction to rGO is obtained by different protocols that give variable surface oxygen functionalization. Furthermore, in composites and polymeric mixtures, these groups interact and vary their availability at the interface, where cells and bacteria can adhere. For this reason, a precise quantification of surface groups would be highly desirable in this

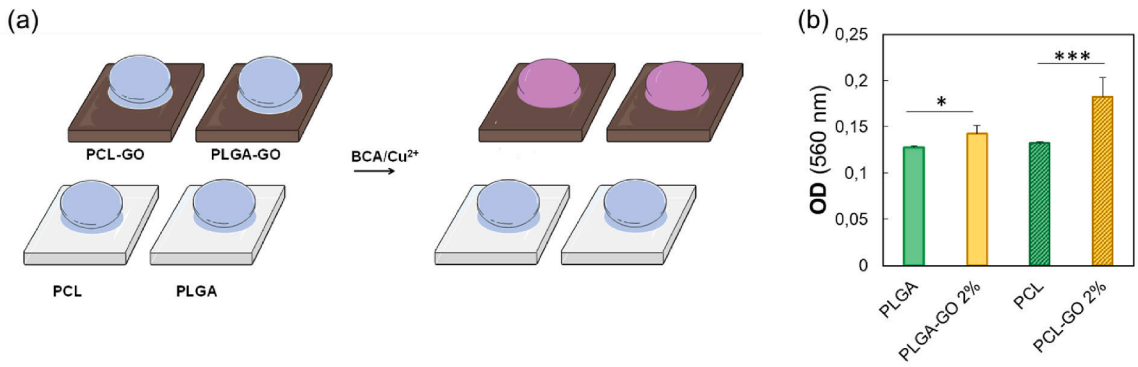

Fig. 5. Graphene Oxide-based composites (GO-1) reaction with BCA on surface (a) and visible light absorption with OD spectroscopy(b).

kind of systems. Despite the difficulty in attaining absolute values of concentrations of the different oxygenated groups in GO layers confined at the surface of a polymeric sample, we demonstrated the possibility to assess their availability and effect in the reaction with Cu^{2+}. More specifically, our method is based on the GO ability to reduce copper and the following colorimetric reaction associated to the interaction of Cu^{1+} and BCA.

We have shown how the development of color is directly proportional to the amount of oxygenated surface groups of graphene, both in terms of graphene material mass concentration and oxidation degree of GO. This property unlocks a quick and easy tool that can be used in laboratories to evaluate the oxygenated groups accessibility at the surface of composite graphene-based scaffolds for biomedical applications. Further investigations are nonetheless required to render this method able to precisely quantify the oxygenated functional groups in graphene oxide materials, e.g. via theoretical modelling of the reaction path of Cu^{2+} reduction exerted by GO.

CRediT authorship contribution statement

Valentina Palmieri: Conceptualization, Funding acquisition, Methodology, Writing – original draft, Writing – review & editing. **Francesco Amato:** Data curation, Formal analysis. **Andrea Giacomo Marrani:** Conceptualization, Data curation, Funding acquisition, Project administration, Resources, Writing – original draft, Writing – review & editing. **Ginevra Friggeri:** Data curation, Formal analysis. **Giordano Perini:** Formal analysis. **Alberto Augello:** Data curation, Formal analysis. **Marco De Spirito:** Project administration, Resources. **Massimiliano Papi:** Conceptualization, Funding acquisition, Project administration, Resources, Writing – review & editing.

Declaration of Competing Interest

The authors declare that they have no known competing financial interests or personal relationships that could have appeared to influence the work reported in this paper.

Data availability

Data will be made available on request.

Acknowledgement

Funding

This research has received funding from AIRC under IG 2019—ID. 23124 project, from the Italian Ministry of Health, GR-2019-12370086, and under FLAGERA JTC2019 MARGO Project. The authors declare no conflict of interest.

References

[1] T.M. Magne, T. de Oliveira Vieira, L.M.R. Alencar, F.F.M. Junior, S. Gemini-Piperni, S.V. Carneiro, L.M.U.D. Fechine, R.M. Freire, K. Golokhvast, P. Metrangolo, Graphene and Its Derivatives: Understanding the Main Chemical and Medicinal Chemistry Roles for Biomedical Applications, *J. Nanostructure Chem.* (2021) 1–35.

[2] R. Di Santo, E. Quagliarini, S. Palchetti, D. Pozzi, V. Palmieri, G. Perini, M. Papi, A. L. Capriotti, A. Laganà, G. Caracciolo, Microfluidic-Generated Lipid-Graphene Oxide Nanoparticles for Gene Delivery, Appl. Phys. Lett. (2019) 114 (23), https://doi.org/10.1063/1.5100932.

[3] V. Palmieri, F. Sciandra, M. Bozzi, M. De Spirito, M. Papi, 3D Graphene Scaffolds for Skeletal Muscle Regeneration: Future Perspectives, Front. Bioeng. Biotechnol. (2020) 8.

[4] V. Palmieri, W. Lattanzi, G. Perini, A. Augello, M. Papi, M. De Spirito, 3D-Printed Graphene for Bone Reconstruction. 7 (2) (2D Mater. 2020,), 022004.

[5] L. Stobinski, B. Lesiak, A. Malolepszy, M. Mazurkiewicz, B. Mierzwa, J. Zemek, P. Jiricek, I. Bieloshapka, Graphene Oxide and Reduced Graphene Oxide Studied by the XRD, TEM and Electron Spectroscopy Methods, J. Electron Spectros. Relat. Phenomena 195 (2014) 145–154, https://doi.org/10.1016/j.elspec.2014.07.003.

[6] D.R. Dreyer, A.D. Todd, C.W. Bielawski, Harnessing the Chemistry of Graphene Oxide, Chem. Soc. Rev. 43 (15) (2014) 5288–5301, https://doi.org/10.1039/c4cs00060a.

[7] V. Palmieri, G. Perini, M. De Spirito, M. Papi, Graphene Oxide Touches Blood:. In Vivo Interactions of Bio-Coronated 2D Materials, Nanoscale Horizons 4 (2) (2019) 464–471, https://doi.org/10.1039/c8nh00318a.

[8] E.D. Sitsanidis, J. Schirmer, A. Lampinen, K.K. Mentel, V.M. Hiltunen, V. Ruokolainen, A. Johansson, P. Myllyperkiö, M. Nissinen, M. Pettersson, Tuning Protein Adsorption on Graphene Surfacesvialaser-Induced Oxidation, Nanoscale Adv. 3 (7) (2021) 2065–2074, https://doi.org/10.1039/d0na01028f.

[9] V. Palmieri, M. De Spirito, M. Papi, Nanofeatures of Orthopedic Implant Surfaces, Future Medicine (2021).

[10] W.C. Lee, C.H.Y.X. Lim, H. Shi, L.A.L. Tang, Y. Wang, C.T. Lim, K.P. Loh, Origin of Enhanced Stem Cell Growth and Differentiation on Graphene and Graphene Oxide, ACS Nano 5 (9) (2011) 7334–7341, https://doi.org/10.1021/nn202190c.

[11] V. Palmieri, M. Barba, L. Di Pietro, S. Gentilini, M.C. Braidotti, C. Ciancico, F. Bugli, G. Ciasca, R. Larciprete, W. Lattanzi, C. Conti, M. Papi, Reduction and Shaping of Graphene-Oxide by Laser-Printing for Controlled Bone Tissue Regeneration and Bacterial Killing. 5 (1) (2D Mater. 2018,), https://doi.org/10.1088/2053-1583/aa9ca7.

[12] V. Palmieri, F. Bugli, M.C. Lauriola, M. Cacaci, R. Torelli, G. Ciasca, C. Conti, M. Sanguinetti, M. Papi, M. De Spirito, Bacteria Meet Graphene: Modulation of Graphene Oxide Nanosheet Interaction with Human Pathogens for Effective Antimicrobial Therapy, ACS Biomater. Sci. Eng. 3 (4) (2017) 619–627, https://doi.org/10.1021/acsbiomaterials.6b00812.

[13] P.C. Henriques, A.T. Pereira, A.L. Pires, A.M. Pereira, F.D. Magalhães, I. C. Gonçalves, Graphene Surfaces Interaction with Proteins, Bacteria, Mammalian Cells, and Blood Constituents: The Impact of Graphene Platelet Oxidation and Thickness, ACS Appl. Mater. Interfaces 12 (18) (2020) 21020–21035, https://doi.org/10.1021/acsami.9b21841.

[14] Z. Shahryari, M. Yeganeh, K. Gheisari, B. Ramezanzadeh, A Brief Review of the Graphene Oxide-Based Polymer Nanocomposite Coatings: Preparation, Characterization, and Properties, *Journal of Coatings Technology and Research*. Springer (July 1, 2021,) 945–969, https://doi.org/10.1007/s11998-021-00488-8.

[15] E.L.K. Chng, M. Pumera, Solid-State Electrochemistry of Graphene Oxides: Absolute Quantification of Reducible Groups Using Voltammetry, Chem. - An Asian J. 6 (11) (2011) 2899–2901, https://doi.org/10.1002/asia.201100464.

[16] F. De Maio, E. Rosa, G. Perini, A. Augello, B. Niccolini, F. Ciaiola, G. Santarelli, F. Sciandra, M. Bozzi, M. Sanguinetti, 3D-Printed Graphene Polylactic Acid Devices Resistant to SARS-CoV-2: Sunlight-Mediated Sterilization of Additive Manufactured Objects, Carbon N. Y. 194 (2022) 34–41.

[17] Otieno, B. A.; Krause, C. E.; Rusling, J. F. Bioconjugation of Antibodies and Enzyme Labels onto Magnetic Beads. In *Methods in enzymology*; Elsevier, 2016; Vol. 571, pp 135–150.

[18] D.C. Marcano, D.V. Kosynkin, J.M. Berlin, A. Sinitskii, Z. Sun, A. Slesarev, L. B. Alemany, W. Lu, J.M. Tour, Improved Synthesis of Graphene Oxide, ACS Nano 4 (8) (2010) 4806–4814.
[19] J. Chen, Y. Li, L. Huang, C. Li, G. Shi, High-Yield Preparation of Graphene Oxide from Small Graphite Flakes via an Improved Hummers Method with a Simple Purification Process, Carbon N. Y. 81 (2015) 826–834.
[20] W.S. Hummers Jr, R.E. Offeman, Preparation of Graphitic Oxide, J. Am. Chem. Soc. 80 (6) (1958) 1339.
[21] S. Guo, S. Garaj, A. Bianco, C. Ménard-Moyon, Controlling Covalent Chemistry on Graphene Oxide, Nat. Rev. Phys. 4 (4) (2022) 247–262.
[22] Silverstein, R. M.; Webster, F. X.; Kiemle, D. J. Silverstein-Spectrometric Identification of Organic Compounds 7th Ed. *State Univ. New York, Coll. Environ. Sci. For.* **2005**.
[23] G. Speranza, L. Minati, The Surface and Bulk Core Lines in Crystalline and Disordered Polycrystalline Graphite, Surf. Sci. 600 (19) (2006) 4438–4444.
[24] K.C. Prince, I. Ulrych, M. Peloi, B. Ressel, V. Chab, C. Crotti, C. Comicioli, Core-Level Photoemission from Graphite, Phys. Rev. B 62 (11) (2000) 6866.
[25] V. Palmieri, E.A. Dalchiele, G. Perini, A. Motta, M. De Spirito, R. Zanoni, A. G. Marrani, M. Papi, Biocompatible N-Acetyl Cysteine Reduces Graphene Oxide and Persists at the Surface as a Green Radical Scavenger, Chem. Commun. 55 (29) (2019) 4186–4189, https://doi.org/10.1039/C9CC00429G.
[26] A.G. Marrani, A.C. Coico, D. Giacco, R. Zanoni, F.A. Scaramuzzo, R. Schrebler, D. Dini, M. Bonomo, E.A. Dalchiele, Integration of Graphene onto Silicon through Electrochemical Reduction of Graphene Oxide Layers in Non-Aqueous Medium, Appl. Surf. Sci. 445 (2018) 404–414, https://doi.org/10.1016/j.apsusc.2018.03.147.
[27] A.G. Marrani, A.C. Coico, D. Giacco, R. Zanoni, A. Motta, R. Schrebler, D. Dini, D. Di Girolamo, E.A. Dalchiele, Flexible Interfaces between Reduced Graphene Oxide and Indium Tin Oxide/Polyethylene Terephthalate for Advanced Optoelectronic Devices, ACS Appl, Nano Mater, 2019.
[28] A.G. Marrani, A. Motta, V. Palmieri, G. Perini, M. Papi, E.A. Dalchiele, R. Schrebler, R. Zanoni, A Comparative Experimental and Theoretical Study of the Mechanism of Graphene Oxide Mild Reduction by Ascorbic Acid and N-Acetyl Cysteine for Biomedical Applications, Mater. Adv. 1 (8) (2020) 2745–2754.
[29] A.G. Marrani, R. Zanoni, R. Schrebler, E.A. Dalchiele, Toward Graphene/Silicon Interface via Controlled Electrochemical Reduction of Graphene Oxide, J. Phys. Chem. C 121 (10) (2017) 5675–5683, https://doi.org/10.1021/acs.jpcc.7b00749.
[30] A.G. Marrani, A. Motta, F. Amato, R. Schrebler, R. Zanoni, E.A. Dalchiele, Effect of Electrolytic Medium on the Electrochemical Reduction of Graphene Oxide on Si (111) as Probed by XPS, Nanomaterials 12 (1) (2021) 43.
[31] C.-Y. Lin, C.-E. Cheng, S. Wang, H.W. Shiu, L.Y. Chang, C.-H. Chen, T.-W. Lin, C.-S. Chang, F.-S.-S. Chien, Synchrotron Radiation Soft X-Ray Induced Reduction in Graphene Oxide Characterized by Time-Resolved Photoelectron Spectroscopy, J. Phys. Chem. C 119 (23) (2015) 12910–12915, https://doi.org/10.1021/jp512055g.
[32] Larciprete, R.; Lacovig, P.; Gardonio, S.; Baraldi, A.; Lizzit, S. Atomic Oxygen on Graphite : Chemical Characterization and Thermal Reduction . *J. Phys. Chem. C* **2012**, *116*, 9900–9908. https://doi.org/dx.doi.org/10.1021/jp2098153.
[33] D. You, K. Li, W. Guo, G. Zhao, C. Fu, Poly (Lactic-Co-Glycolic Acid)/graphene Oxide Composites Combined with Electrical Stimulation in Wound Healing: Preparation and Characterization, Int. J. Nanomedicine 14 (2019) 7039.
[34] A. Seyedsalehi, L. Daneshmandi, M. Barajaa, J. Riordan, C.T. Laurencin, Fabrication and Characterization of Mechanically Competent 3D Printed Polycaprolactone-Reduced Graphene Oxide Scaffolds, Sci. Rep. 10 (1) (2020) 1–14.
[35] K. Yin, D. Chu, X. Dong, C. Wang, J.-A. Duan, J. He, Femtosecond Laser Induced Robust Periodic Nanoripple Structured Mesh for Highly Efficient Oil–water Separation, Nanoscale 9 (37) (2017) 14229–14235.
[36] Y. He, L. Wang, T. Wu, Z. Wu, Y. Chen, K. Yin, Facile Fabrication of Hierarchical Textures for Substrate-Independent and Durable Superhydrophobic Surfaces, Nanoscale 14 (26) (2022) 9392–9400.
[37] P. Matteini, F. Tatini, L. Cavigli, S. Ottaviano, G. Ghini, R. Pini, Graphene as a Photothermal Switch for Controlled Drug Release, Nanoscale 6 (14) (2014) 7947–7953.